# Development and Thermal Performance Modeling and Analysis of a Serpentine and Spiral Tube Solar Thermal Collector

1st Alaa Husain University of Bahrain Isa Town, Bahrain a.husaindz@gmail.com

2<sup>nd</sup> Abdulla Abdulla University of Bahrain Isa Town, Bahrain a.jassim202@gmail.com

3<sup>rd</sup> Muaath Essam dept. Mechanical Engineering dept. Mechanical Engineering dept. Mechanical Engineering dept. Mechanical Engineering University of Bahrain Isa Town, Bahrain muaathesssam@gmail.com

4th Abdul Waheed Badar University of Bahrain Isa Town, Bahrain awbadar@uob.edu.bh

Abstract-Solar thermal collectors are the main energy generation component of any solar-driven heating and cooling system type and configuration. The presented work aims to design and develop two configurations of liquid solar thermal collectors consisting of a serpentine and spiral tube attached to a flat absorber sheet to conduct performance evaluation and comparison to demonstrate solar energy's potential for potential low- to medium-temperature thermal applications. The work was executed in three phases. The first phase was to mathematically model the working of the liquid solar thermal collector to analyze their thermal performance for a range of input parameters. The energy balance equations were formulated and solved iteratively to compute the energy gain of the fluid and estimate the unknown fluid, absorber plate, and glazing temperatures. The influence of a wide range of parameters, including inlet fluid temperature, fluid flow rate, solar radiation intensity, ambient temperature, etc., was studied on the collector's performance factors. In the second phase, both solar collector components were manufactured and/or procured from the local market, and the collectors were assembled. In the final phase, experiments were performed by measuring different physical parameters, such as fluid and absorber plate temperature and mass flow rate, to estimate and document the thermal performance of the solar collectors. The results showed that the spiral tube design performs better than the serpentine-type collector, achieving an average thermal efficiency of 48.2%, about 9% higher than the serpentine collector.

# I. INTRODUCTION

Energy for water heating and particularly for air conditioning across the whole oil-rich Middle East region heavily depends on fossil fuels. Huge amounts of oil, gas, and coal are burned to power the area, with residential use accounting for half of the energy demand, mostly due to air conditioning. With the depletion of fossil fuels and increasing concerns about environmental and climate-related issues, exploiting solar energy for air conditioning and power generation is the need of the day. The potential of solar energy with scratching heat during summer in this region for meeting heating and/or cooling demands is evident.

Among several types of solar thermal collectors, flat plate solar collectors (FPSCs) with different flow configurations are quite extensively being studied and used in practice for

various applications, such as domestic water and/or space heating [1]-[3], space cooling systems [4], etc. A prior study shows an innovative spiral FPSC demonstrated 21.4% higher thermal efficiency than conventional FPSCs [5], though replicating these conditions is challenging. Another paper found serpentine FPSCs had a higher temperature rise than spiral ones [6], but Bahrain's unique conditions may affect these results. Additionally, the design proposed for our project differs significantly from the models discussed.

### II. MATHEMATICAL MODELLING

The primary goal of the research is to enhance efficiency, which is a key indicator of a collector's output. Efficiency is determined by the ratio of useful energy harnessed to the total solar energy incident on the collector plate. It is influenced by several factors, such as the product of the glazing's transmittance and the absorber plate's absorptance, as well as the intensity of solar irradiance. These factors are essential in calculating the efficiency and other related parameters of solar collectors [5].

Given the intricate geometry of the novel spiral-shaped collector, empirical experimentation will be prioritized. Nonetheless, a mathematical model has been developed for the Serpentine FPSC for detailed analysis.

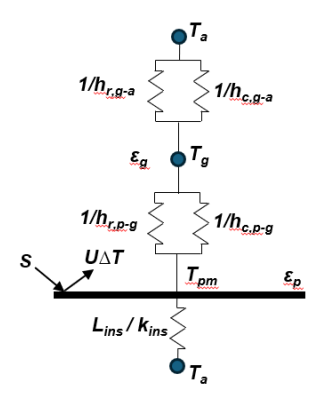


Fig. 1. Thermal Network Schematics.

The value of absorbed solar irradiance on the absorber plate is calculated by (1).

$$S = (\tau \propto)G \tag{1}$$

The thermal energy lost from the absorber plate to the cold ambient is computed by estimating overall heat transfer coefficient  $(U_L)$ , which further consists of convective and conductive heat transfers between the absorber plate and glazing and between glazing and ambient (see Figure 1)

The convective heat transfer (H.T.) coefficient between the ambient environment and the glass cover is determined using (2). Additionally, the radiative H.T. coefficient is computed in accordance with (3). Subsequently, these values are utilized to ascertain the thermal resistance between the glass cover and the ambient, as delineated in (4).

$$h_{c,q-a} = 5.7 + 3.8V_{air} (2)$$

$$h_{r,q-a} = \varepsilon_q \sigma \left( (T_q + T_a) \left( T_q^2 + T_a^2 \right) \right) \tag{3}$$

$$R_{g-a} = \frac{1}{h_{c,g-a} + h_{r,g-a}} \tag{4}$$

To determine the convection heat transfer coefficient between the glass cover and the absorber plate, it is vital to calculate the air temperature as the average of the plate and cover temperatures. This allows for the computation of the thermophysical properties of the air, which in turn facilitates the determination of the Nusselt number.

$$T_{air} = \frac{T_p + T_g}{2} \tag{5}$$

$$R_a = \frac{g \cdot \Pr}{T_a \cdot v} \cdot (T_p - T_g) \cdot L \tag{6}$$

$$Nu = \left\{ 1 + 1.44 \left[ 1 - \frac{1708 \cdot \sin(1.8\beta)^{1.6}}{R_a \cos(\beta)} \right]$$

$$\left[ 1 - \frac{1708}{R_a \cos(\beta)} \right]^+ + \left[ \sqrt[3]{\frac{R_a \cos(\beta)}{5830}} - 1 \right]^+ \right\}$$
 (7)

$$h_{c,p-g} = \frac{Nu \cdot k}{L} \tag{8}$$

As the surfaces do not emit radiation to their own surface, they both have a view factor of 1. This results in the following radiation H.T. resistance:

$$h_{r,p-g} = \frac{\sigma(T_p + T_g) \left( (T_p)^2 + (T_g)^2 \right)}{\left( \frac{1}{\varepsilon_p} \right) + \left( \frac{1}{\varepsilon_g} \right) - 1} \tag{9}$$

$$R_{p-g} = \frac{1}{h_{c,p-g} + h_{r,p-g}} \tag{10}$$

Using the thermal resistances between the absorber plate, glass cover, and ambient, the top thermal loss coefficient can be calculated as:

$$U_t = \frac{1}{R_{p-q} + R_{q-a}} \tag{11}$$

Due to the insulation below the absorber plate, the bottom thermal loss is approximately 10% of the top thermal loss. The bottom thermal loss coefficient is calculated as:

$$U_b = \frac{k_{ins}}{L_{ins}} \tag{12}$$

The overall thermal loss coefficient is the sum of the top and bottom thermal losses:

$$U_L = U_t + U_b \tag{13}$$

Similar to air, water's mean temperature is calculated and used to find the fluid's flow properties and convection H.T. coefficient and the relevant equations are shown below.

$$T_{mf} = \frac{T_{fi} + T_{fo}}{2} \tag{14}$$

$$v_w = \frac{\dot{m}_w}{\rho_w \cdot A_0} \tag{15}$$

$$Re_w = \frac{\rho_w \cdot v_w \cdot D_{fi}}{\mu_w} \tag{16}$$

$$Pr_w = \frac{\mu_w C_{p,w}}{k_w} \tag{17}$$

$$C_{f,w} = \left[0.79 \cdot \log \left(Re_w\right)^{-1.64}\right]^{-2}$$
 (18)

$$Nu_w = 0.023 \cdot Pr_w^{0.4} \cdot Re_w^{0.8} \tag{19}$$

$$h_{fi} = \frac{Nu_w \cdot k_{fw}}{D_{fi}} \tag{20}$$

### A. Fin Efficiency

The efficiency of a straight fin with rectangular profile can be expressed as follows:

$$F = \frac{\tanh\left(\frac{m_f * (W_f - D_{fo})}{2}\right)}{\frac{m_f * (W_f - D_{fo})}{2}}$$
(21)

$$m_f = \sqrt{\frac{U_L}{k_{copper}\delta}} \tag{22}$$

The collector's efficiency factor (F') is the ratio between the actual useful heat collection rate and the useful heat collection rate that would occur if the collector's absorbing plate were at the fluid temperature. It can be expressed as:

$$F' = \frac{\frac{1}{U_L}}{W_f \left\{ \frac{1}{U_L[D_f + (W_f - D_f)F]} + \frac{1}{\pi D_{fi} h_{fi}} \right\}}$$
(23)

Collector Flow Factor (F") is given as:

$$F'' = \frac{\dot{m}_w * C_{p,w}}{A_C * U_L * F' * \left[ 1 - \exp\left( -\frac{A_C * U_L * F'}{\dot{m}_w * C_{p,w}} \right) \right]}$$
(24)

The Heat Removal Factor  $(F_R)$  for serpentine tube configuration can be calculated based on the equation provided by Zhang and Lavan [7]. For the calculation of the dimensionless factors  $F_1$  to  $F_6$ , refer to [7].

$$F_R = F_1 F_3 F_5 \left[ \frac{2F_4}{F_6 \exp\left(-\frac{\sqrt{1 - F_2^2}}{F_3}\right) + F_5} - 1 \right]$$
 (25)

Net heat gain of the solar collector in the form of mean plate & inlet fluid temperatures are given as:

$$Q_{w,p} = A_C * [S - U_L * (T_p - T_a)]$$
 (26)

$$Q_{u,f} = A_C * F_R * [S - U_L * (T_{fi} - T_a)]$$
 (27)

The temperatures of the absorber plate, fluid, glass cover, and outlet fluid are computed as [7]:

$$T_{mf} = T_{fi} + \frac{\frac{Q_{w,p}}{A_C}}{F_R * U_L} (1 - F'')$$
 (28)

$$T_p = T_{fi} + \frac{\frac{Q_{w,p}}{A_C}}{F_R * U_L} (1 - F_R)$$
 (29)

$$T_g = T_p - [U_t (T_p - T_a)] h_{c,p-g} + h_{r,p-g}$$
 (30)

$$T_{fo} = \frac{Q_{u,f}}{\dot{m}_w * C_{p,w}} + T_{fi}$$
 (31)

Theoretical efficiency can be expressed by the ratio of useful heat gain to the total input energy:

$$\eta = \frac{Q_{u,f}}{A_C * G} \tag{32}$$

The mathematical model was created using MATLAB to simulate the performance of a flat plate collector, focusing on heat transfer, fluid temperatures, and plate temperatures under various conditions. Initial assumptions of mean plate, glass and mean fluid temperatures serve as placeholders for unknown values, allowing the model to start and enabling sensitivity analysis by varying key parameters to identify critical parameters.

TABLE I ITERATED PARAMETERS

Iterated Parameters	
Plate Temperature (°C)	100
Glass Temperature (°C)	35
Inlet Temperature (°C)	20
Outlet Temperature (°C)	30

#### III. MODELING RESULTS & DISCUSSION

After completion of the initial phase of design and simulation of the solar thermal collector, optimal conditions and parameters were obtained by plotting performance curves over a select range of values against specific variables.

TABLE II
OPERATION CONDITIONS

Operation Conditions	
Ambient Temperature (°C)	30
Solar Irradiation (W/m <sup>2</sup> )	1000
Gravity (m/s <sup>2</sup> )	9.807
Air Velocity (m/s)	3

#### A. Mass Flowrate

Figure 2 describes the behavior of the serpentine FPSC with the variation of mass flow rate at increasing collector efficiency. Observations indicate a sudden increase in efficiency at approximately 0.025 Kg/s, this is a result of a change in fluid flow pattern from laminar to turbulent. Based on the curve the optimal value within the laminar region is approximately 0.01 Kg/s.

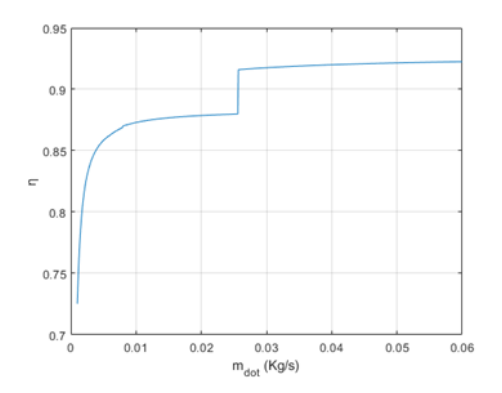


Fig. 2. Efficiency versus mass flow rate.

#### B. Fluid Outlet Temperature

Figure 3 demonstrates the behavior of a serpentine solar thermal collector with the variation of mass flow rate at exponentially decreasing fluid outlet temperature. Observations indicate a sudden decrease in fluid outlet temperature at approximately 0.005 Kg/s.

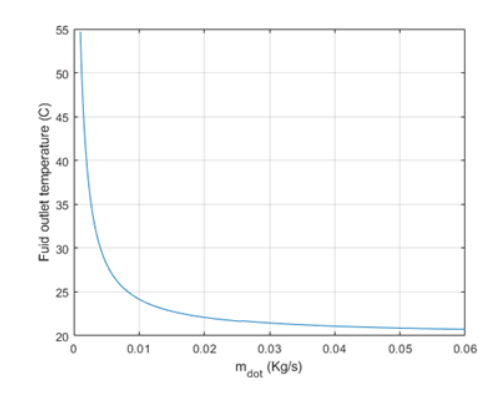


Fig. 3. Fluid outlet temperature versus mass flow rate.

### C. Insulation Thickness

The influence of of varying isulation on  $U_L$  is depicted in Figure 4. It is evident that  $U_L$  diminishes as the insulation thickness increases. However, beyond a threshold of 0.035 m, further augmentation in insulation thickness yields a negligible impact on  $U_L$ .

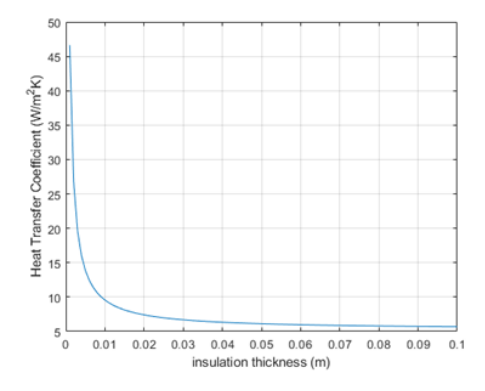


Fig. 4. Heat transfer coefficient (W/m<sup>2</sup>K) versus insulation thickness.

## IV. MANUFACTURING & FABRICATION

The collectors' CAD models are shown below in Figures 5 & 6.

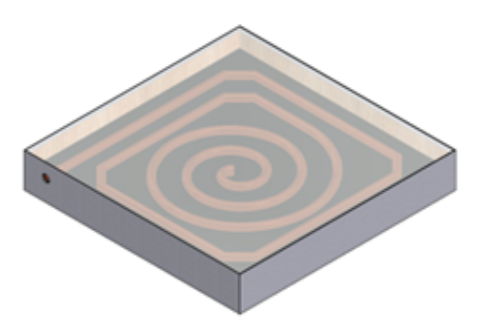


Fig. 5. Spiral FPSC 3D Model.

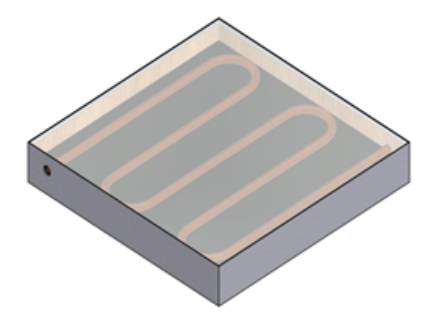


Fig. 6. Serpentine FPSC 3D Model.

The materials utilized for each component are consistent for both FPSCs and are detailed in Table III below.

The stand has been constructed with a fixed inclination, matching Bahrain's latitude of approximately 26°.

TABLE III MATERIALS USED IN EACH FPSC

Item	Material
Absorber Plate	Galvanized Steel
Tubes	Copper
Insulation	Extruded Polystyrene
Glazing	Tempered Glass
Collector Box	Galvanized Steel

The fabrication of each solar thermal collector followed a standard step-by-step process:

- 1) Box Manufacturing
- 2) Tube Shaping
- 3) Welding
- 4) Painting
- 5) Assembly & Glazing

The dimensional details of individual components are given in Table IV.

Pictorial views of fabricated collectors are shown in Figures 7 & 8



Fig. 7. Fabricated Spiral FPSC.



Fig. 8. Fabricated Serpentine FPSC.

### V. EXPERIMENTATION RESULTS & DISCUSSION

The newly designed Spiral FPSC and its counterpart, the Serpentine FPSC, underwent rigorous testing on May 17th and 21st, 2024, respectively.

TABLE IV
SPECIFICATIONS OF SERPENTINE AND SPIRAL FPSC

Specification	Dimensions		Unit
Specification	Serpentine FPSC	Spiral FPSC	Ullit
Collector Occupied Space	50*50*8	50*50*8	cm <sup>3</sup>
Collector Box Thickness	2	2	mm
Absorber Plate Thickness	1	1	mm
Absorber Plate Area	0.25	0.25	$m^2$
Glazing Thickness	6	6	mm
Tube Length	3.5	3.5	m
Tube Spacing	8	Variable	cm
Tube Outer Diameter	0.625	0.625	in
Tube Inner Diameter	0.569	0.569	in
Back Insulation Thickness	40	40	mm
Conductivity of Insulation	0.024	0.024	W/mK

During the testing period, the ambient temperatures recorded were  $40^{\circ}$ C on the first day (May 17th) and  $41^{\circ}$ C on the second day (May 21st). The mass flow rate was determined to be in the range of 0.01-0.02 kg/s. DS18B20 temperature sensors having error margins of  $\pm 0.5^{\circ}$ C were used to measure the inlet & outlet fluid temperatures along with the absorber plate temperature (see Figure 9).

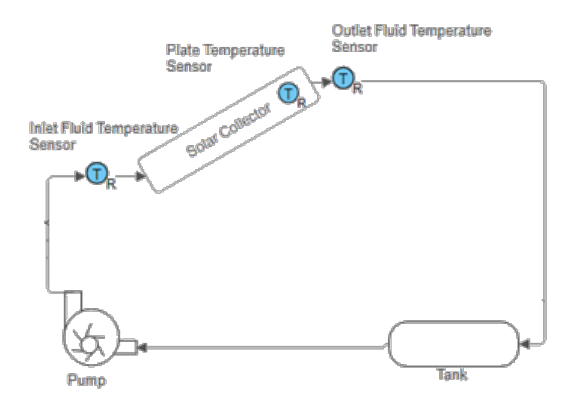


Fig. 9. Experimental Setup Schematics.

# A. Spiral FPSC Experimental Performance

Figures 10, 11, and 14 illustrate the experimental performance of the Spiral FPSC. As shown in Figure 10, the inlet and outlet temperatures are increasing, resulting in a reduction in efficiency, as evident in Figure 14. Figure 11 reveals that  $T_{avg}$  (average fluid temperature) and  $T_p$  (plate temperature) are reaching a plateau, indicating that the system is approaching a steady state. The mean efficiency was calculated to be approximately 48.2%.

### B. Serpentine FPSC Experimental Performance

Similarly, Figures 12-14 show the performance of the Serpentine FPSC. In Figure 12, the inlet and outlet temperatures also approach equilibrium, leading to a reduction in efficiency, as seen in Figure 14. Figure 13 demonstrates that  $T_{avg}$  and  $T_p$  are reaching a plateau, indicating a steady state similar to the Spiral FPSC. The mean efficiency for the Serpentine FPSC was calculated to be approximately 39.5%.

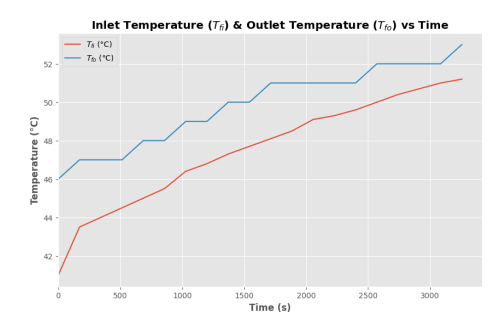


Fig. 10. Spiral FPSC - Inlet & Outlet Temperatures Through Time.

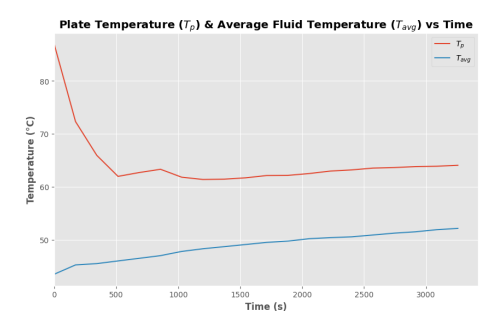


Fig. 11. Spiral FPSC - Relationship b/w Plate & Average Fluid Temperatures.

These observations suggest that both the Spiral and Serpentine FPSCs exhibit comparable performance characteristics under their respective test conditions, as both achieved mean fluid temperatures in the range of 50°C. Although the Spiral FPSC resulted in 10% higher mean efficiency than the Serpentine FPSC, more detailed analysis is required to ascertain this outcome by repeating experiments for a wide range of operating conditions.

## VI. CONCLUSION

In this work, the thermal performance of two configurations of flat plate solar collectors (FPSCs) (i.e., serpentine and spiral types) were evaluated and compared. An analytical model of the serpentine-type FPSC was developed and solved iteratively to study the influence of design parameters, such as mass flow rate, insulation thickness, etc. Two prototype models

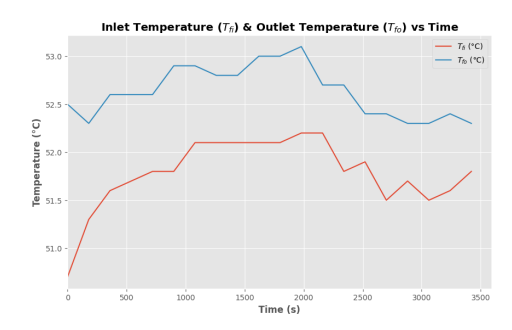


Fig. 12. Serpentine FPSC - Inlet & Outlet Temperatures Through Time.

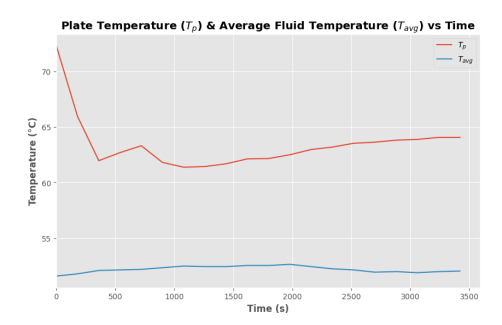


Fig. 13. Serpentine FPSC - Plate & AVG Fluid Temperature Relationship.

of serpentine and spiral FPSCs were developed and tested. Results of the experimentation revealed that the novel spiralshaped FPSC has shown superior performance. However, further experimentation is required to reaffirm this conclusion.

## NOMENCLATURE

Absorptivity  $\alpha$ β Tilt angle (Rad) δ Thickness of Plate (m) **Emissivity**  $\epsilon$ Efficiency (%)  $\eta$ **Dimensionless Constant**  $\gamma$  $\kappa$ **Dimensionless Constant** Dynamic Viscosity  $(Ns/m^2)$  $\mu$ Density  $(kg/m^3)$ ρ Stefan-Boltzmann Constant  $(W/(m^2 \cdot K^4))$  $\sigma$ Transmittance

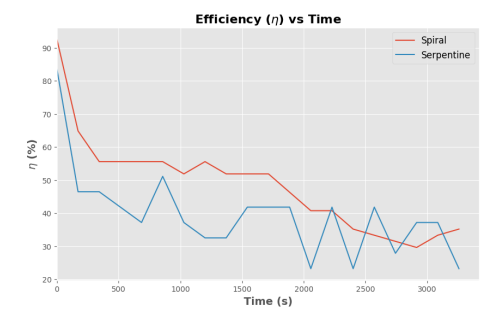


Fig. 14. Serpentine & Spiral FPSCs Performance Comparison.

- Area  $(m^2)$ A $C_b$ Bond Conductance  $(W/m \cdot K)$ Fanning Friction Factor  $C_f$ DDiameter (m) DOutside Diameter (m) FStandard Fin Efficiency for Straight Fins F'Collector Efficiency Factor F''Collector Flow Factor  $F_1$ Dimensionless Parameter  $F_2$ **Dimensionless Parameter** Dimensionless Parameter  $F_3$  $F_4$ Dimensionless Parameter  $F_5$ Dimensionless Parameter **Dimensionless Parameter**  $F_6$ Collector Heat Removed Factor  $F_R$ GSolar Irradiance  $(W/m^2)$ Gravitational Acceleration  $(m/s^2)$ gConvection H.T. Coefficient  $(W/(m^2 \cdot K))$  $h_c$ Radiation H.T. Coefficient  $(W/(m^2 \cdot K))$  $h_r$ Fluid to tube H.T. Coefficient  $(W/(m^2 \cdot K))$  $h_{fi}$ Thermal Conductivity  $(W/(m \cdot K))$ kLLength (m) m-Constant  $m_f$ Nusselt Number NuPrPrandtl Number QThermal Energy (J) RThermal resistance (K/W)
  - RaRayleigh Number
  - ReReynolds Number SEnergy Absorbed  $(W/m^2)$ TTemperature (K)
  - Overall H.T. Coefficient  $(W/(m^2 \cdot K))$ U
  - VVelocity (m/s) Velocity (m/s) v

#### REFERENCES

- [1] O. Ibrahim, F. Fardoun, R. Younes, and H. Louahlia-Gualous, "Review of water-heating systems: General selection approach based on energy and environmental aspects," Building and Environment, vol. 72, pp. 259–286, 2014.
- [2] S. A. Khan, A. Badar, M. Siddiqui, M. S. ul Haq, and F. Butt, "Modeling and comparative assessment of solar thermal systems for space and water heating: Liquid water versus air-based systems," Journal of Renewable and Sustainable Energy (AIP), vol. 15, no. 6, 2023.
- [3] Y. Tian and C. Y. Zhao, "A review of solar collectors and thermal energy storage in solar thermal applications," Applied Energy, vol. 104, pp. 538-553, 2013.
- [4] Q. Al-Yasiri, M. Szabó, and M. Arıcı, "A review on solar-powered cooling and air-conditioning systems for building applications," Energy Reports, vol. 8, pp. 2888-2907, 2022.
- Verma, K. Sharma, [5] S. K. N. K. Gupta, P. Soni, and N. Upadhyay, ""performance comparison of innovative spiral shaped solar collector design with conventional flat plate solar collector"," Energy, vol. 194, p. 116853, 2020. [Online]. Available: https://www.sciencedirect.com/science/article/pii/S0360544219325484
- [6] A. S. Abdulsitar and N. A. Hasan, "Comparison between spiral and serpentine flow solar water heater," Journal of University of Babylon for Engineering Sciences, vol. 30, no. 2, pp. 89-99, 2022.
- [7] J. A. Duffie and W. A. Beckman, Solar Engineering of Thermal Processes, 4th ed. Wiley, 2013.